FERMILAB-PUB-11-350-E

A search for resonant production of $t\bar{t}$ pairs in 4.8 fb^{-1} of integrated luminosity of $p\bar{p}$ collisions at $\sqrt{s} = 1.96$ TeV

T. Aaltonen,[21] B. Álvarez González[x],[9] S. Amerio,[40] D. Amidei,[32] A. Anastassov[v],[15] A. Annovi,[17] J. Antos,[12] G. Apollinari,[15] J.A. Appel,[15] T. Arisawa,[54] A. Artikov,[13] J. Asaadi,[49] W. Ashmanskas,[15] B. Auerbach,[57] A. Aurisano,[49] F. Azfar,[39] W. Badgett,[15] T. Bae,[25] A. Barbaro-Galtieri,[26] V.E. Barnes,[44] B.A. Barnett,[23] P. Barria[ff],[42] P. Bartos,[12] M. Bauce[dd],[40] F. Bedeschi,[42] D. Beecher,[28] S. Behari,[23] G. Bellettini[ee],[42] J. Bellinger,[56] D. Benjamin,[14] A. Beretvas,[15] A. Bhatti,[46] M. Binkley*,[15] D. Bisello[dd],[40] I. Bizjak[jj],[28] K.R. Bland,[5] B. Blumenfeld,[23] A. Bocci,[14] A. Bodek,[45] D. Bortoletto,[44] J. Boudreau,[43] A. Boveia,[11] L. Brigliadori[cc],[6] C. Bromberg,[33] E. Brucken,[21] J. Budagov,[13] H.S. Budd,[45] K. Burkett,[15] G. Busetto[dd],[40] P. Bussey,[19] A. Buzatu,[31] A. Calamba,[10] C. Calancha,[29] S. Camarda,[4] M. Campanelli,[28] M. Campbell,[32] F. Canelli[11],[15] B. Carls,[22] D. Carlsmith,[56] R. Carosi,[42] S. Carrillo[l],[16] S. Carron,[15] B. Casal[j],[9] M. Casarsa,[50] A. Castro[cc],[6] P. Catastini,[20] D. Cauz,[50] V. Cavaliere,[22] M. Cavalli-Sforza,[4] A. Cerri[e],[26] L. Cerrito[q],[28] Y.C. Chen,[1] M. Chertok,[7] G. Chiarelli,[42] G. Chlachidze,[15] F. Chlebana,[15] K. Cho,[25] D. Chokheli,[13] W.H. Chung,[56] Y.S. Chung,[45] M.A. Ciocci[ff],[42] A. Clark,[18] C. Clark,[55] G. Compostella[dd],[40] M.E. Convery,[15] J. Conway,[7] M.Corbo,[15] M. Cordelli,[17] C.A. Cox,[7] D.J. Cox,[7] F. Crescioli[ee],[42] J. Cuevas[x],[9] R. Culbertson,[15] D. Dagenhart,[15] N. d'Ascenzo[u],[15] M. Datta,[15] P. de Barbaro,[45] M. Dell'Orso[ee],[42] L. Demortier,[46] M. Deninno,[6] F. Devoto,[21] M. d'Errico[dd],[40] A. Di Canto[ee],[42] B. Di Ruzza,[15] J.R. Dittmann,[5] M. D'Onofrio,[27] S. Donati[ee],[42] P. Dong,[15] M. Dorigo,[50] T. Dorigo,[40] K. Ebina,[54] A. Elagin,[49] A. Eppig,[32] R. Erbacher,[7] S. Errede,[22] N. Ershaidat[bb],[15] R. Eusebi,[49] H.C. Fang,[26] S. Farrington,[39] M. Feindt,[24] J.P. Fernandez,[29] R. Field,[16] G. Flanagan[s],[44] R. Forrest,[7] M.J. Frank,[5] M. Franklin,[20] J.C. Freeman,[15] Y. Funakoshi,[54] I. Furic,[16] M. Gallinaro,[46] J.E. Garcia,[18] A.F. Garfinkel,[44] P. Garosi[ff],[42] H. Gerberich,[22] E. Gerchtein,[15] V. Giakoumopoulou,[3] P. Giannetti,[42] K. Gibson,[43] C.M. Ginsburg,[15] N. Giokaris,[3] P. Giromini,[17] G. Giurgiu,[23] V. Glagolev,[13] D. Glenzinski,[15] M. Gold,[35] D. Goldin,[49] N. Goldschmidt,[16] A. Golossanov,[15] G. Gomez,[9] G. Gomez-Ceballos,[30] M. Goncharov,[30] O. González,[29] I. Gorelov,[35] A.T. Goshaw,[14] K. Goulianos,[46] S. Grinstein,[4] C. Grosso-Pilcher,[11] R.C. Group[55],[15] J. Guimaraes da Costa,[20] Z. Gunay-Unalan,[33] C. Haber,[26] S.R. Hahn,[15] E. Halkiadakis,[48] A. Hamaguchi,[38] J.Y. Han,[45] F. Happacher,[17] K. Hara,[51] D. Hare,[48] M. Hare,[52] R.F. Harr,[55] K. Hatakeyama,[5] C. Hays,[39] M. Heck,[24] J. Heinrich,[41] M. Herndon,[56] S. Hewamanage,[5] A. Hocker,[15] W. Hopkins[f],[15] D. Horn,[24] S. Hou,[1] R.E. Hughes,[36] M. Hurwitz,[11] U. Husemann,[57] N. Hussain,[31] M. Hussein,[33] J. Huston,[33] G. Introzzi,[42] M. Iori[hh],[47] A. Ivanov[o],[7] E. James,[15] D. Jang,[10] H.J. Jang,[25] B. Jayatilaka,[14] E.J. Jeon,[25] S. Jindariani,[15] W. Johnson,[7] M. Jones,[44] K.K. Joo,[25] S.Y. Jun,[10] T.R. Junk,[15] T. Kamon,[49] P.E. Karchin,[55] A. Kasmi,[5] Y. Kato[n],[38] W. Ketchum,[11] J. Keung,[41] V. Khotilovich,[49] B. Kilminster,[15] D.H. Kim,[25] H.S. Kim,[25] J.E. Kim,[25] M.J. Kim,[17] S.B. Kim,[25] S.H. Kim,[51] Y.K. Kim,[11] Y.J. Kim,[25] N. Kimura,[54] M. Kirby,[15] K. Knoepfel,[15] K. Kondo*,[54] D.J. Kong,[25] J. Konigsberg,[16] A.V. Kotwal,[14] M. Kreps,[24] J. Kroll,[41] D. Krop,[11] M. Kruse,[14] V. Krutelyov[c],[49] T. Kuhr,[24] M. Kurata,[51] S. Kwang,[11] A.T. Laasanen,[44] S. Lami,[42] S. Lammel,[15] M. Lancaster,[28] R.L. Lander,[7] K. Lannon[w],[36] A. Lath,[48] G. Latino[ee],[42] T. LeCompte,[2] E. Lee,[49] H.S. Lee,[11] J.S. Lee,[25] S.W. Lee[z],[49] S. Leo[ee],[42] S. Leone,[42] J.D. Lewis,[15] A. Limosani[r],[14] C.-J. Lin,[26] J. Linacre,[39] M. Lindgren,[15] E. Lipeles,[41] A. Lister,[18] D.O. Litvintsev,[15] C. Liu,[43] H. Liu,[53] Q. Liu,[44] T. Liu,[15] S. Lockwitz,[57] A. Loginov,[57] D. Lucchesi[dd],[40] J. Lueck,[24] P. Lujan,[26] P. Lukens,[15] G. Lungu,[46] J. Lys,[26] R. Lysak,[12] R. Madrak,[15] K. Maeshima,[15] P. Maestro[ff],[42] S. Malik,[46] G. Manca[a],[27] A. Manousakis-Katsikakis,[3] F. Margaroli,[47] C. Marino,[24] M. Martínez,[4] K. Matera,[22] M.E. Mattson,[55] A. Mazzacane,[15] P. Mazzanti,[6] K.S. McFarland,[45] P. McIntyre,[49] R. McNulty[i],[27] A. Mehta,[27] P. Mehtala,[21] C. Mesropian,[46] T. Miao,[15] D. Mietlicki,[32] A. Mitra,[1] H. Miyake,[51] S. Moed,[15] N. Moggi,[6] M.N. Mondragon[l],[15] C.S. Moon,[25] R. Moore,[15] M.J. Morello[gg],[42] J. Morlock,[24] P. Movilla Fernandez,[15] A. Mukherjee,[15] Th. Muller,[24] P. Murat,[15] M. Mussini[cc],[6] J. Nachtman[m],[15] Y. Nagai,[51] J. Naganoma,[54] I. Nakano,[37] A. Napier,[52] J. Nett,[49] C. Neu,[53] M.S. Neubauer,[22] J. Nielsen[d],[26] L. Nodulman,[2] S.Y. Noh,[25] O. Norniella,[22] E. Nurse,[28] L. Oakes,[39] S.H. Oh,[14] Y.D. Oh,[25] I. Oksuzian,[53] T. Okusawa,[38] R. Orava,[21] L. Ortolan,[4] S. Pagan Griso[dd],[40] C. Pagliarone,[50] E. Palencia[e],[9] V. Papadimitriou,[15] A.A. Paramonov,[2] J. Patrick,[15] G. Pauletta[ii],[50] M. Paulini,[10] C. Paus,[30] D.E. Pellett,[7] A. Penzo,[50] T.J. Phillips,[14] G. Piacentino,[42] E. Pianori,[41] J. Pilot,[36] K. Pitts,[22] C. Plager,[8] L. Pondrom,[56] S. Poprocki[f],[15] K. Potamianos,[44] O. Poukhov*,[13] F. Prokoshin[aa],[13] A. Pranko,[15] F. Ptohos[g],[17] G. Punzi[ee],[42] A. Rahaman,[43] V. Ramakrishnan,[56] N. Ranjan,[44] I. Redondo,[29] P. Renton,[39] M. Rescigno,[47] T. Riddick,[28] F. Rimondi[cc],[6] L. Ristori[44],[15] A. Robson,[19] T. Rodrigo,[9] T. Rodriguez,[41] E. Rogers,[22] S. Rolli[h],[52] R. Roser,[15] F. Rubbo,[42] F. Ruffini[ff],[42] A. Ruiz,[9] J. Russ,[10] V. Rusu,[15] A. Safonov,[49] W.K. Sakumoto,[45] Y. Sakurai,[54] L. Santi[ii],[50] K. Sato,[51] V. Saveliev[u],[15] A. Savoy-Navarro[y],[15]

P. Schlabach,[15] A. Schmidt,[24] E.E. Schmidt,[15] M.P. Schmidt*,[57] T. Schwarz,[15] L. Scodellaro,[9] A. Scribano[ff],[42] F. Scuri,[42] A. Sedov,[44] S. Seidel,[35] Y. Seiya,[38] A. Semenov,[13] F. Sforza[ff],[42] S.Z. Shalhout,[7] T. Shears,[27] P.F. Shepard,[43] M. Shimojima[t],[51] M. Shochet,[11] I. Shreyber-Tecker,[34] A. Simonenko,[13] P. Sinervo,[31] A. Sissakian*,[13] K. Sliwa,[52] J.R. Smith,[7] F.D. Snider,[15] A. Soha,[15] V. Sorin,[4] P. Squillacioti[ff],[42] M. Stancari,[15] R. St. Denis,[19] B. Stelzer,[31] O. Stelzer-Chilton,[31] D. Stentz[v],[15] J. Strologas,[35] G.L. Strycker,[32] Y. Sudo,[51] A. Sukhanov,[15] I. Suslov,[13] K. Takemasa,[51] Y. Takeuchi,[51] J. Tang,[11] M. Tecchio,[32] P.K. Teng,[1] J. Thom[f],[15] J. Thome,[10] G.A. Thompson,[22] E. Thomson,[41] D. Toback,[49] S. Tokar,[12] K. Tollefson,[33] T. Tomura,[51] D. Tonelli,[15] S. Torre,[17] D. Torretta,[15] P. Totaro,[40] M. Trovato[gg],[42] Y. Tu,[41] F. Ukegawa,[51] S. Uozumi,[25] A. Varganov,[32] F. Vázquez[l],[16] G. Velev,[15] C. Vellidis,[15] M. Vidal,[44] I. Vila,[9] R. Vilar,[9] J. Vizán,[9] M. Vogel,[35] G. Volpi,[17] P. Wagner,[41] R.L. Wagner,[15] T. Wakisaka,[38] R. Wallny,[8] S.M. Wang,[1] A. Warburton,[31] D. Waters,[28] W.C. Wester III,[15] D. Whiteson[b],[41] A.B. Wicklund,[2] E. Wicklund,[15] S. Wilbur,[11] F. Wick,[24] H.H. Williams,[41] J.S. Wilson,[36] P. Wilson,[15] B.L. Winer,[36] P. Wittich[f],[15] S. Wolbers,[15] H. Wolfe,[36] T. Wright,[32] X. Wu,[18] Z. Wu,[5] K. Yamamoto,[38] T. Yang,[15] U.K. Yang[p],[11] Y.C. Yang,[25] W.-M. Yao,[26] G.P. Yeh,[15] K. Yi[m],[15] J. Yoh,[15] K. Yorita,[54] T. Yoshida[k],[38] G.B. Yu,[14] I. Yu,[25] S.S. Yu,[15] J.C. Yun,[15] A. Zanetti,[50] Y. Zeng,[14] and S. Zucchelli[cc6]

(CDF Collaboration[†])

[1]*Institute of Physics, Academia Sinica, Taipei, Taiwan 11529, Republic of China*
[2]*Argonne National Laboratory, Argonne, Illinois 60439, USA*
[3]*University of Athens, 157 71 Athens, Greece*
[4]*Institut de Fisica d'Altes Energies, ICREA, Universitat Autonoma de Barcelona, E-08193, Bellaterra (Barcelona), Spain*
[5]*Baylor University, Waco, Texas 76798, USA*
[6]*Istituto Nazionale di Fisica Nucleare Bologna,* [cc]*University of Bologna, I-40127 Bologna, Italy*
[7]*University of California, Davis, Davis, California 95616, USA*
[8]*University of California, Los Angeles, Los Angeles, California 90024, USA*
[9]*Instituto de Fisica de Cantabria, CSIC-University of Cantabria, 39005 Santander, Spain*
[10]*Carnegie Mellon University, Pittsburgh, Pennsylvania 15213, USA*
[11]*Enrico Fermi Institute, University of Chicago, Chicago, Illinois 60637, USA*
[12]*Comenius University, 842 48 Bratislava, Slovakia; Institute of Experimental Physics, 040 01 Kosice, Slovakia*
[13]*Joint Institute for Nuclear Research, RU-141980 Dubna, Russia*
[14]*Duke University, Durham, North Carolina 27708, USA*
[15]*Fermi National Accelerator Laboratory, Batavia, Illinois 60510, USA*
[16]*University of Florida, Gainesville, Florida 32611, USA*
[17]*Laboratori Nazionali di Frascati, Istituto Nazionale di Fisica Nucleare, I-00044 Frascati, Italy*
[18]*University of Geneva, CH-1211 Geneva 4, Switzerland*
[19]*Glasgow University, Glasgow G12 8QQ, United Kingdom*
[20]*Harvard University, Cambridge, Massachusetts 02138, USA*
[21]*Division of High Energy Physics, Department of Physics,*
University of Helsinki and Helsinki Institute of Physics, FIN-00014, Helsinki, Finland
[22]*University of Illinois, Urbana, Illinois 61801, USA*
[23]*The Johns Hopkins University, Baltimore, Maryland 21218, USA*
[24]*Institut für Experimentelle Kernphysik, Karlsruhe Institute of Technology, D-76131 Karlsruhe, Germany*
[25]*Center for High Energy Physics: Kyungpook National University,*
Daegu 702-701, Korea; Seoul National University, Seoul 151-742,
Korea; Sungkyunkwan University, Suwon 440-746,
Korea; Korea Institute of Science and Technology Information,
Daejeon 305-806, Korea; Chonnam National University, Gwangju 500-757,
Korea; Chonbuk National University, Jeonju 561-756, Korea
[26]*Ernest Orlando Lawrence Berkeley National Laboratory, Berkeley, California 94720, USA*
[27]*University of Liverpool, Liverpool L69 7ZE, United Kingdom*
[28]*University College London, London WC1E 6BT, United Kingdom*
[29]*Centro de Investigaciones Energeticas Medioambientales y Tecnologicas, E-28040 Madrid, Spain*
[30]*Massachusetts Institute of Technology, Cambridge, Massachusetts 02139, USA*
[31]*Institute of Particle Physics: McGill University, Montréal, Québec,*
Canada H3A 2T8; Simon Fraser University, Burnaby, British Columbia,
Canada V5A 1S6; University of Toronto, Toronto, Ontario,
Canada M5S 1A7; and TRIUMF, Vancouver, British Columbia, Canada V6T 2A3
[32]*University of Michigan, Ann Arbor, Michigan 48109, USA*
[33]*Michigan State University, East Lansing, Michigan 48824, USA*
[34]*Institution for Theoretical and Experimental Physics, ITEP, Moscow 117259, Russia*
[35]*University of New Mexico, Albuquerque, New Mexico 87131, USA*
[36]*The Ohio State University, Columbus, Ohio 43210, USA*

[37] Okayama University, Okayama 700-8530, Japan
[38] Osaka City University, Osaka 588, Japan
[39] University of Oxford, Oxford OX1 3RH, United Kingdom
[40] Istituto Nazionale di Fisica Nucleare, Sezione di Padova-Trento, [dd] University of Padova, I-35131 Padova, Italy
[41] University of Pennsylvania, Philadelphia, Pennsylvania 19104, USA
[42] Istituto Nazionale di Fisica Nucleare Pisa, [ee] University of Pisa,
[ff] University of Siena and [gg] Scuola Normale Superiore, I-56127 Pisa, Italy
[43] University of Pittsburgh, Pittsburgh, Pennsylvania 15260, USA
[44] Purdue University, West Lafayette, Indiana 47907, USA
[45] University of Rochester, Rochester, New York 14627, USA
[46] The Rockefeller University, New York, New York 10065, USA
[47] Istituto Nazionale di Fisica Nucleare, Sezione di Roma 1,
[hh] Sapienza Università di Roma, I-00185 Roma, Italy
[48] Rutgers University, Piscataway, New Jersey 08855, USA
[49] Texas A&M University, College Station, Texas 77843, USA
[50] Istituto Nazionale di Fisica Nucleare Trieste/Udine,
I-34100 Trieste, [ii] University of Udine, I-33100 Udine, Italy
[51] University of Tsukuba, Tsukuba, Ibaraki 305, Japan
[52] Tufts University, Medford, Massachusetts 02155, USA
[53] University of Virginia, Charlottesville, Virginia 22906, USA
[54] Waseda University, Tokyo 169, Japan
[55] Wayne State University, Detroit, Michigan 48201, USA
[56] University of Wisconsin, Madison, Wisconsin 53706, USA
[57] Yale University, New Haven, Connecticut 06520, USA

We search for resonant production of $t\bar{t}$ pairs in 4.8 fb^{-1} integrated luminosity of $p\bar{p}$ collision data at $\sqrt{s} = 1.96$ TeV in the lepton+jets decay channel, where one top quark decays leptonically and the other hadronically. A matrix element reconstruction technique is used; for each event a probability density function (pdf) of the $t\bar{t}$ candidate invariant mass is sampled. These pdfs are used to construct a likelihood function, whereby the cross section for resonant $t\bar{t}$ production is estimated, given a hypothetical resonance mass and width. The data indicate no evidence of resonant production of $t\bar{t}$ pairs. A benchmark model of leptophobic $Z' \to t\bar{t}$ is excluded with $m_{Z'} < 900$ GeV/c^2 at 95% confidence level.

PACS numbers: 13.85.Rm, 14.65.Ha, 14.70.Hp, 14.70.Pw, 14.80.Rt, 14.80.Tt

Many theories of physics beyond the standard model (SM) predict additional vector bosons (e.g. Z'). These include (but are not limited to) extended gauge theories (e.g. SO(10)), Kaluza–Klein states of the gluon or of Z bosons, axigluons, and topcolor [1–10]. Previous analyses of Tevatron data have excluded such narrow resonances with masses less than 725 GeV/c^2 [11–14].

In this Letter we describe a search for narrow resonant states decaying to top–antitop pairs in proton–antiproton collisions using the CDF II detector at the Tevatron at Fermilab. We discuss the experimental signature of resonant $t\bar{t}$ production and how we are to distinguish it from standard model $t\bar{t}$ production. We describe the reconstruction technique used in this analysis and the statistical tests we perform in examining the data for any sign of the hypothetical resonant production, and we describe the systematic uncertainties related to this analysis. Observing no evidence for resonant production of $t\bar{t}$ pairs, we set upper limits on the cross section times branching ratio for resonant $t\bar{t}$ production.

At the Tevatron, the $t\bar{t}$ pair–production cross section has been measured with great precision: $\sigma_{p\bar{p}\to t\bar{t}} = 7.70 \pm 0.52$ pb [15]. However, this degree of precision leaves open the possibility that non–SM physics gives rise to a

*Deceased
†With visitors from [a] Istituto Nazionale di Fisica Nucleare, Sezione di Cagliari, 09042 Monserrato (Cagliari), Italy, [b] University of CA Irvine, Irvine, CA 92697, USA, [c] University of CA Santa Barbara, Santa Barbara, CA 93106, USA, [d] University of CA Santa Cruz, Santa Cruz, CA 95064, USA, [e] CERN, CH-1211 Geneva, Switzerland, [f] Cornell University, Ithaca, NY 14853, USA, [g] University of Cyprus, Nicosia CY-1678, Cyprus, [h] Office of Science, U.S. Department of Energy, Washington, DC 20585, USA, [i] University College Dublin, Dublin 4, Ireland, [j] ETH, 8092 Zurich, Switzerland, [k] University of Fukui, Fukui City, Fukui Prefecture, Japan 910-0017, [l] Universidad Iberoamericana, Mexico D.F., Mexico, [m] University of Iowa, Iowa City, IA 52242, USA, [n] Kinki University, Higashi-Osaka City, Japan 577-8502, [o] Kansas State University, Manhattan, KS 66506, USA, [p] University of Manchester, Manchester M13 9PL, United Kingdom, [q] Queen Mary, University of London, London, E1 4NS, United Kingdom, [r] University of Melbourne, Victoria 3010, Australia, [s] Muons, Inc., Batavia, IL 60510, USA, [t] Nagasaki Institute of Applied Science, Nagasaki, Japan, [u] National Research Nuclear University, Moscow, Russia, [v] Northwestern University, Evanston, IL 60208, USA, [w] University of Notre Dame, Notre Dame, IN 46556, USA, [x] Universidad de Oviedo, E-33007 Oviedo, Spain, [y] CNRS-IN2P3, Paris, F-75252 France, [z] Texas Tech University, Lubbock, TX 79609, USA, [aa] Universidad Tecnica Federico Santa Maria, 110v Valparaiso, Chile, [bb] Yarmouk University, Irbid 211-63, Jordan, [jj] On leave from J. Stefan Institute, Ljubljana, Slovenia

fraction of the total $t\bar{t}$ production.

We search for a heavy vector boson decaying to $t\bar{t}$ in the final state where one top quark decays semileptonically ($t \to \ell\nu b$) and the other hadronically ($t \to q\bar{q}'b$) [16] by examining the $t\bar{t}$ invariant mass spectrum of candidate events, where the event kinematics have been reconstructed by applying the SM QCD "Matrix Element" for $t\bar{t}$ production and decay [13]. The observed spectrum is then compared to templates – models of signal (i.e., $Z' \to t\bar{t}$) and background processes (e.g. SM $t\bar{t}$, W+jets, WW/WZ) in an unbinned maximum–likelihood fit. By fitting the data to these models, we extract upper limits on the $Z' \to t\bar{t}$ cross section times branching ratio. We consider scenarios where the Z' width is 1.2% of the pole mass (this has been the benchmark scenario for narrow–resonance searches in $t\bar{t}$ enriched samples [6]).

The CDF detector is a general purpose, azimuthally and forward-backward symmetric multipurpose collider detector. A detailed description can be found in Ref. [17]; here we summarize details of detector components important to this analysis. The transverse momenta ($p_{\rm T}$) and track parameters of charged particles are measured by an eight-layer silicon strip detector [18–20] and a 96-layer drift chamber (COT) [21], both within a 1.4 T magnetic field. The COT provides tracking coverage with high efficiency for $|\eta| < 1$ [22]. Electromagnetic [23] and hadronic [24] calorimeters surround the tracking system. They are segmented in a projective tower geometry and measure the energies of charged and neutral particles in the central region ($|\eta| < 1.1$). A plug tile calorimeter covers the forward region ($1.1 < |\eta| < 3.6$). Each calorimeter has an electromagnetic shower profile detector positioned at the shower maximum. The calorimeters are surrounded by muon drift chambers [25]. The central muon detectors comprise four layers of drift chambers which cover the region $|\eta| \leq 0.6$. Forward muons, with $0.6 < |\eta| < 1.0$, are detected by an additional four layers of drift chambers. Gas Čerenkov counters [26] measure the average number of inelastic $p\bar{p}$ collisions per beam–crossing and thereby determine the beam luminosity.

We select $t\bar{t}$ candidates in data corresponding to an integrated luminosity of 4.8 fb^{-1} in the lepton+jets channel [27] by requiring one isolated charged lepton — an electron (reconstructed using the central electromagnetic calorimeter) or a muon (reconstructed with the central or forward muon detectors).

Primary leptons must have rapidity $|\eta| < 1$. Electrons must have transverse energy $E_{\rm T} > 20$ GeV and muons must have transverse momentum $p_{\rm T} > 20$ GeV/c. Four or more central jets ($|\eta| < 2$) with $E_{\rm T} > 20$ GeV are also required. One of these jets must have a secondary vertex displaced from the primary event vertex such that it is "tagged" by the SECVTX algorithm [28] as being consistent with the decay of a long–lived b-hadron. Jets with b-tags are restricted to $|\eta| < 1$. Large missing transverse energy [29] is also required, $\not\!\!E_{\rm T} > 20$ GeV. Jets corrected [30] for multiple $p\bar{p}$ interactions in the event, non-uniformities in the calorimeter response along η and any non-linearity and energy loss in the uninstrumented regions of the calorimeters. The $\not\!\!E_{\rm T}$ is corrected for the primary vertex location and for any high–$p_{\rm T}$ muons in the event.

component	4 jets	≥ 5 jets
non-W	46.1 ± 35.7	15.7 ± 12.2
Z+light flavor	6.4 ± 0.5	1.6 ± 0.1
W+light flavor	32.9 ± 8.5	7.4 ± 3.1
$Wb\bar{b}$	51.5 ± 12.6	12.4 ± 3.7
$Wc\bar{c}$	27.7 ± 6.6	7.3 ± 2.1
Wcj	14.0 ± 3.3	3.0 ± 0.9
single top	8.9 ± 0.4	1.4 ± 0.0
diboson	9.1 ± 0.6	2.4 ± 0.1
total non–$t\bar{t}$	196.6 ± 39.5	51.2 ± 13.3
SM $t\bar{t}$	667.1 ± 61.8	225.2 ± 21.0

TABLE I. Estimate of sample composition in terms of signal and background.

	central $e^{\pm}$	central $\mu^{\pm}$	forward $\mu^{\pm}$
4 jets, 1 tag	480	221	131
4 jets, ≥ 2 tags	110	33	21
≥ 5 jets, 1 tag	164	81	41
≥ 5 jets, ≥ 2 tags	47	21	16

TABLE II. Number of events observed in each subsample for data corresponding to an integrated luminosity of 4.8 fb^{-1}.

The contribution of non–$t\bar{t}$ backgrounds satisfying this selection has been derived in precision measurements of the $t\bar{t}$ production cross section [27], these are tabulated in Table I. Also shown is the expected SM $t\bar{t}$ content, given the event selection. However, in this analysis the SM $t\bar{t}$ content is estimated as the difference between the number of observed events and the estimate of resonant $t\bar{t}$ events plus non–$t\bar{t}$ background events. Table II indicates the number of events observed in each of the subsamples considered in this analysis.

For each candidate event, we apply the $t\bar{t}$ hypothesis – the observed event kinematics are mapped to the parton level using the information available in the SM QCD "Matrix Element" for $t\bar{t}$ production and decay [13]. By constraining the event kinematics to the hypothetical matrix element, we can reconstruct with enhanced precision any kinematic quantity which can be expressed in terms of the parton momenta. In this analysis, we reconstruct the $t\bar{t}$ invariant mass probability density function (pdf) for each event.

The probability for $t\bar{t}$ production and decay, given p, the four–momenta of the decay products of the $t\bar{t}$ system, is

$$\pi(p|m_t) = \frac{1}{\sigma(m_t)} \int {\rm d}z_a {\rm d}z_b f_k(z_a) f_l(z_b) {\rm d}\sigma_{kl}(p|m_t, z_a, z_b), \quad (1)$$

where $f_k(z_a)$ and $f_l(z_b)$ are the parton density func-

tions for incoming gluons or quarks with flavor k and l, with z–components of parton momenta, z_a and z_b. $\mathrm{d}\sigma_{kl}(p|m_t, z_a, z_b)$ is the differential cross section – it is proportional to the squared SM matrix element for $t\bar{t}$ production and decay. In this analysis, we fix the top-quark mass, $m_t = 172.5$ GeV/c^2.

Any quantity which can be expressed as a function of the momenta of the top decay products can be estimated as a probability density. We consider the invariant mass of the top–antitop pair, and derive the following pdf of x, the reconstructed $t\bar{t}$ invariant mass:

$$\rho(x) \equiv \int \sum_k \pi(p_k|m_t) W(j|p_k) \delta(x - \mathbb{M}(p_k)) \mathrm{d}p_k. \quad (2)$$

$\mathbb{M}(p_k)$ is the invariant mass of the top-antitop pair, given parton configuration p_k, and $W(j|p_k)$ is a transfer function which maps the observed jets j to the parton level. The sum is over the number of permutations, or jet–parton assignments, possible given the observed event.

The transfer functions $W(j|p_k)$ used in Eq. (2) are estimates of the primary parton energy corresponding to the observed jet E_{T}. These estimates are derived from Monte Carlo simulation, where jets are matched to partons within $\Delta R \equiv \sqrt{\Delta\eta + \Delta\phi} < 0.15$. No other jets or partons may be within $\Delta R < 0.6$ of the jet/parton match. We separate the response function into 10 GeV jet–energy bins and into five bins of jet pseudo-rapidity.

The matrix-element calculation produces a probability density function of the reconstructed $t\bar{t}$ invariant mass for each event. We use this sampled pdf as the observable in a likelihood calculation. The probability for an event in sample i is a function of the signal fraction f_{sig} in the sample:

$$P_i(f_{\mathrm{sig}}) = f_{\mathrm{sig}} P_{\mathrm{sig},i} + (1 - f_{\mathrm{sig}}) P_{\mathrm{bg},i}. \quad (3)$$

Here we regard the hypothetical $Z' \to t\bar{t}$ component as signal and SM $t\bar{t}$ and non–$t\bar{t}$ processes as background. The cross section σ for $Z' \to t\bar{t}$ and the signal fraction are proportional,

$$f_{\mathrm{sig}} = \frac{1}{n} \sigma \sum_{i=1}^{N_s} L_i A_i \quad (4)$$

where n is the total number of events observed, $N_s = 3 \times 2 \times 2 = 12$ is the number of samples [31], and L_i and A_i are, respectively, the integrated luminosity and absolute signal acceptance. The signal and background probabilities $P_{\mathrm{sig},i}$ and $P_{\mathrm{bg},i}$ are, according to their templates,

$$P_{\mathrm{sig},i} = \int T_{\mathrm{sig},i}(x) \rho(x) \mathrm{d}x, \quad (5)$$

and

$$P_{\mathrm{bg},i} = \int T_{\mathrm{bg},i}(x) \rho(x) \mathrm{d}x. \quad (6)$$

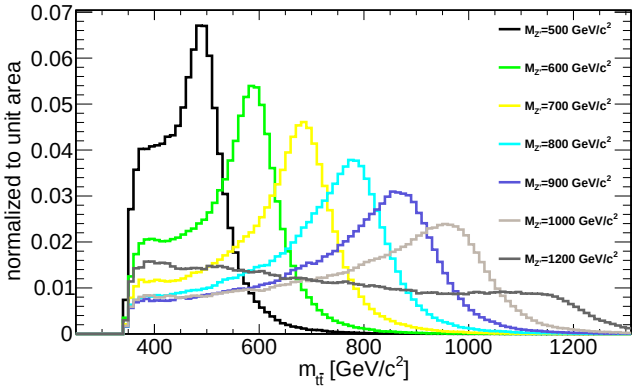

FIG. 1. Signal templates—summed over b-tag multiplicity, jet multiplicity and primary lepton type.

These templates, $T_{\mathrm{sig},i}$ and $T_{\mathrm{bg},i}$, are the summed event–by–event pdfs from each of the model components (e.g. the Monte Carlo models of SM $t\bar{t}$, W+jets, etc.). The templates and the per–event pdfs are normalized to unit area:

$$T_{c,i}(x) = \frac{1}{N_c} \sum_{j=1}^{N_c} \rho_j(x) \quad (7)$$

$$\int \rho(x) dx \equiv 1 \quad (8)$$

where $T_{c,i}$ is the template for component c in sample i and N_c is the total number of events used to model component c.

Templates for each model component are constructed by summing the per–event probability densities. In Fig. 1 we show the templates for $Z' \to t\bar{t}$ at several values of the Z' pole mass, reconstructed according to the procedure described above. Note that the mass peak is generally prominent. For the samples where the Z' pole mass is 1000 GeV/c^2 and above, fewer Z' particles are produced on–shell. The off–shell Z' is produced with mass according to the energy available from the parton density functions, but decays to a real $t\bar{t}$ pair. The invariant mass spectrum for on and off–shell $Z' \to t\bar{t}$ depends on the Z' pole mass; we are able to distinguish the Z' mass, given the observed reconstructed $t\bar{t}$ mass spectrum, even in cases where the Z' mass is very large and the Z' is largely produced off–shell.

To model the background components ALPGEN [32] version 2.10 with PYTHIA version 6.2.16 [33] parton showering is used for W+heavy flavor and W+jets. The shape of the $t\bar{t}$ invariant mass at next to leading order (NLO) is softer than the predictions of leading order Monte Carlo codes. To correct for this effect, PYTHIA weighted at the generator level by MCFM [34] (version 5.8) is used to model the SM $t\bar{t}$ component. The QCD "fake" component (where a jet is mis–reconstructed as an electron) is modeled in data, where jets are selected which are

electron–like in their identification variables. Compared to the signal templates (Fig. 1), we notice excellent separation between background and signal shapes.

We write the likelihood simply as the product of the per–event probabilities,

$$L(\sigma) = \prod_{i,j} P_i(\sigma) \cdot G(\nu_j|\overline{\nu}_j, \sigma_j) \quad (9)$$

where G is a Gaussian distribution, ν_j is nuisance parameter j with expectation $\overline{\nu}_j$ and uncertainty σ_j. We include among the nuisance parameters each lepton category acceptance and its error, as well as the lepton trigger efficiencies. SECVTX tagging acceptance is modeled by applying a scale factor to account for differences between data and simulation. This scale factor appears as another nuisance parameter. We integrate over the nuisance parameters to incorporate these systematic effects into the likelihood.

The measurement is affected by uncertainties inherent to our model of the background: the amount of initial– and final–state radiation (ISR and FSR) and the uncertainty on the jet energy scale [30] of the calorimeter contribute most significantly, while systematic uncertainties due to parton distribution function and color–reconnection effects [35, 36] are negligible. While the value of the top quark mass determines the value at which the $t\bar{t}$ invariant mass spectrum rises [10], the shape of the *tail* of the $m_{t\bar{t}}$ spectrum is insensitive to variation of the top mass within its uncertainty. This analysis is sensitive specifically to variations of the tail of the $m_{t\bar{t}}$ spectrum—uncertainty on the value of the top quark mass is not a significant source of systematic error.

We treat systematic uncertainties due to acceptance effects as nuisance parameters (cf. Eq. (9)), while we convolve the likelihood function to include systematic effects due to background model uncertainties.

Background model systematic uncertainties are estimated by evaluating ensemble tests where the experimental circumstances are reproduced and the parameter in question (e.g. initial– or final–state radiation, estimates of background shape or composition) is varied within its error. The resulting distribution of the maximum likelihood estimate of signal cross section form the basis for these estimates of systematic uncertainty. We take the difference in the means of the $+1\sigma$ and -1σ distributions as the error due to the underlying uncertainty at each mass value of the hypothetical resonances considered. The final tabulation of estimated systematic uncertainties for this analysis is given in Table III.

These errors are assumed to be Gaussian in nature. The likelihood of Eq. (9) is convolved with a Gaussian distribution whose width is equal to the quadrature sum of the individual systematic uncertainties:

$$L'(\sigma) = \int_0^\infty G(\sigma, \sigma', \Delta\sigma) L(\sigma') d\sigma'. \quad (10)$$

The distribution of reconstructed $t\bar{t}$ invariant mass observed in the data is shown in Figure 2. This histogram shows the integrated probability density in each $t\bar{t}$ invariant mass bin. For each event we observe a *distribution*; as a consequence any single event can contribute probability density to more than one bin. The data show no indication of resonant $t\bar{t}$ production. Moreover, the distribution observed agrees very well with the background model over five orders of magnitude.

At each value of the Z' pole mass considered we calculate the Bayesian 95% confidence level (C.L.) upper limit on the value of the cross section times branching ratio for Z' production and decay to $t\bar{t}$. This upper limit is the value of cross section times branching ratio which covers 95% of the area under the convolved likelihood, integrating from zero cross section, where a flat prior is

Z' pole mass [GeV/c^2]	$\Delta\sigma$ [pb]
450	0.210
500	0.183
550	0.155
600	0.153
650	0.087
700	0.058
750	0.044
800	0.030
850	0.025
900	0.020
950	0.012
1000	0.014
1100	0.016
1200	0.011
1300	0.029
1400	0.036
1500	0.065

TABLE III. Total background model systematic uncertainties at each of the mass points considered. These values appear as the width of the Gaussian convolved with the likelihood in Eq. (10).

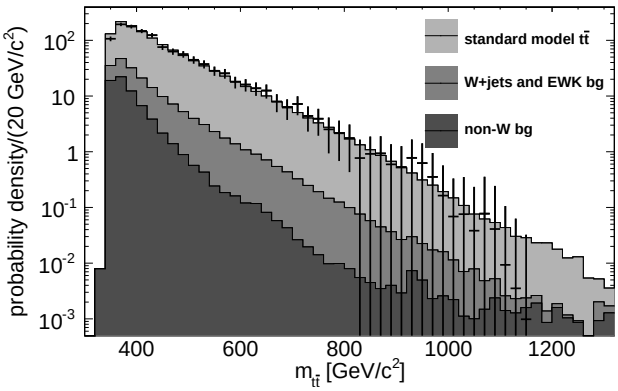

FIG. 2. The histogram of total probability density for the 1366 $t\bar{t}$ candidate events observed in $\mathcal{L} = 4.8$ fb^{-1}.

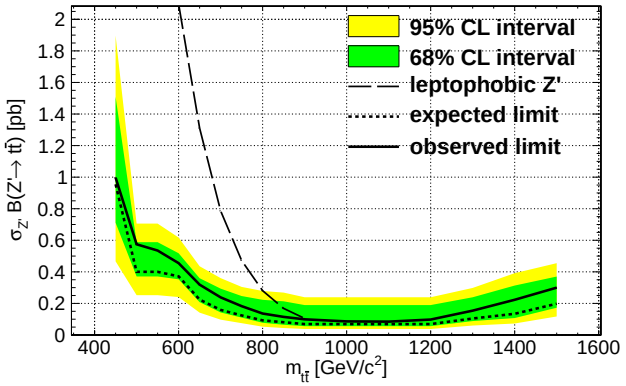

FIG. 3. Expected and observed 95% C.L. upper limit for $\sigma(p\bar{p} \to Z') \times BR(Z' \to t\bar{t})$ for $\mathcal{L} = 4.8$ fb^{-1} of integrated luminosity as a function of reconstructed $t\bar{t}$ invariant mass. The solid line indicates the observed limit. The dashed line indicates the theoretical cross section for a leptophobic Z' [6].

$m_{Z'}$ [GeV/c^2]	Expected limit [pb]	Observed limit [pb]
450	0.954	1.05
500	0.400	0.49
550	0.400	0.46
600	0.371	0.40
650	0.224	0.26
700	0.159	0.20
750	0.123	0.15
800	0.092	0.11
850	0.080	0.10
900	0.068	0.09
950	0.069	0.08
1000	0.069	0.07
1100	0.069	0.07
1200	0.070	0.08
1300	0.104	0.13
1400	0.134	0.18
1500	0.197	0.24

TABLE IV. Expected and observed 95% C.L. limits on the cross section times branching ratio for narrow resonance production.

assumed.

Figure 3 shows the expected and observed limits on the Z' cross section times branching ratio at each mass point considered. These data are also given in tabular form in Table IV. The green band shows the $\pm 1\sigma$ expectation for the null hypothesis, the yellow band the $\pm 2\sigma$ expectation. Also included is a curve indicating the theoretical cross section for a leptophobic Z' [6].

We have searched for narrow resonant states decaying to top–antitop pairs in a sample corresponding to an integrated luminosity of 4.8 fb^{-1} of CDF II data. Events were selected in the lepton + $\geq$ 4 jets topology with at least one jet tagged as coming from a b quark. Monte Carlo samples were used to model the appearance of narrow resonant states decaying to $t\bar{t}$. A matrix–element reconstruction method was applied, and for each event a probability density function of the reconstructed $t\bar{t}$ invariant mass was sampled. This formed the basis for a likelihood fit to extract the cross section times branching ratio for narrow resonance production, where non–$t\bar{t}$ background fractions are constrained according to their best estimates, and SM and resonant $t\bar{t}$ components may vary according to the data. Systematic uncertainties such as those arising from the error on the jet energy scale, or uncertainties on parton distribution functions were incorporated by convolving the likelihood function with a Gaussian with width equal to the estimated uncertainty on the cross section times branching ratio due to the underlying uncertainty. Systematic uncertainties arising from acceptance affects such as trigger efficiencies or scale factors are treated as nuisance parameters in the likelihood function. The benchmark model of a leptophobic Z' [6] is ruled out at 95% C.L. for Z' masses below 900 GeV/c^2.

We thank the Fermilab staff and the technical staffs of the participating institutions for their vital contributions. This work was supported by the U.S. Department of Energy and National Science Foundation; the Italian Istituto Nazionale di Fisica Nucleare; the Ministry of Education, Culture, Sports, Science and Technology of Japan; the Natural Sciences and Engineering Research Council of Canada; the National Science Council of the Republic of China; the Swiss National Science Foundation; the A.P. Sloan Foundation; the Bundesministerium für Bildung und Forschung, Germany; the Korean World Class University Program, the National Research Foundation of Korea; the Science and Technology Facilities Council and the Royal Society, UK; the Institut National de Physique Nucleaire et Physique des Particules/CNRS; the Russian Foundation for Basic Research; the Ministerio de Ciencia e Innovación, and Programa Consolider-Ingenio 2010, Spain; the Slovak R&D Agency; the Academy of Finland; and the Australian Research Council (ARC).

[1] S. Weinberg, Phys. Rev. D **13**, 974 (1976).
[2] S. Dimopoulos and H. Georgi, Nucl. Phys. B **193**, 150 (1981).
[3] C. T. Hill and S. J. Parke, Phys. Rev. D **49**, 4454 (1994).
[4] N. Arkani-Hamed, S. Dimopoulos, and G. R. Dvali, Phys. Lett. B **429**, 263 (1998).
[5] L. Randall and R. Sundrum, Phys. Rev. Lett. **83**, 3370 (1999).
[6] R. M. Harris, C. T. Hill, and S. J. Parke, Fermilab-FN-687, hep-ph/9911288 (1999).

[7] R. S. Chivukula, B. A. Dobrescu, H. Georgi, and C. T. Hill, Phys. Rev. D **59** 75003 (1999).

[8] N. Arkani-Hamed, A. G. Cohen, and H. Georgi, Phys. Lett. B **513**, 232 (2001).

[9] A. L. Fitzpatrick, J. Kaplan, L. Randall, and L. - T. Wang, JHEP **0709**, 013 (2007).

[10] R. Frederix and F. Maltoni, JHEP **0901**, 047 (2009).

[11] V. M. Abazov *et al.* (D0 Collaboration), Phys. Rev. Lett. **92**, 221801 (2004).

[12] T. Aaltonen *et al.* (CDF Collaboration), Phys. Rev. D **77**, 051102 (2008).

[13] T. Aaltonen *et al.* (CDF Collaboration), Phys. Rev. Lett. **100**, 231801 (2008).

[14] V. M. Abazov *et al.* (D0 Collaboration), Phys. Lett. B **668**, 98 (2008).

[15] T. Aaltonen *et al.* (CDF Collaboration), Phys. Rev. Lett. **105**, 012001 (2010).

[16] This is the so-called "lepton+jets" topology. We consider leptonic decays including only final–state electrons and muons.

[17] A. Abulencia *et al.* (CDF Collaboration), J. Phys. G **34**, 2457 (2007).

[18] C. Hill *et al.* (CDF Collaboration), Nucl. Instrum. Methods Phys. Res., Sect. A **530**, 1 (2004).

[19] A. Sill *et al.* (CDF Collaboration), Nucl. Instrum. Methods Phys. Res., Sect. A **447**, 1 (2000).

[20] A. Affolder *et al.* (CDF Collaboration), Nucl. Instrum. Methods Phys. Res., Sect. A **453**, 84 (2000).

[21] T. Affolder *et al.* (CDF Collaboration), Nucl. Instrum. Methods Phys. Res., Sect. A **526**, 249 (2004).

[22] We use a cylindrical coordinate system with its origin in the center of the detector and the downstream proton beam as reference axis, where θ and ϕ are the polar and azimuthal angles, respectively, and pseudo-rapidity is $\eta = -\ln\tan\theta/2$. The transverse energy $E_{\rm T}$ (momentum $p_{\rm T}$) is defined as $E\sin\theta$ ($p\sin\theta$).

[23] L. Balka *et al.* (CDF Collaboration), Nucl. Instrum. Methods Phys. Res., Sect. A **267**, 272 (1988).

[24] S. Bertolucci *et al.*, Nucl. Instrum. Methods Phys. Res., Sect. A **267**, 301 (1988).

[25] G. Ascoli *et al.* (CDF Collaboration), Nucl. Instrum. Methods Phys. Res., Sect. A **268**, 33 (1988).

[26] D. Acosta *et al.* (CDF Collaboration), Nucl. Instrum. Methods Phys. Res., Sect. A **461**, 540 (2001).

[27] T. Aaltonen *et al.* (CDF Collaboration), Phys. Rev. Lett. **105**, 012001 (2010); D. Acosta *et al.*, (CDF Collaboration), Phys. Rev. D **71**, 052003 (2005).

[28] D. Acosta *et al.* (CDF Collaboration), Phys. Rev. D **71**, 052003 (2005).

[29] The missing transverse energy $\vec{\not\!\!E}_T$ is calculated as the negative vector sum of the energy in each calorimeter tower multiplied by a unit vector in the azimuthal direction of the vector sum. $\not\!\!E_{\rm T}$ is defined as the magnitude of $\vec{\not\!\!E}_T$.

[30] A. Bhatti *et al.* (CDF Collaboration), Nucl. Instrum. Meth. A **566** 375 (2006).

[31] The twelve samples are the product of three primary lepton types (central electrons, central muons, and forward muons), two b–tag multiplicities (1 tag, $\geq$ 2 tags), and two jet multiplicities (4 jets, $\geq$ 5 jets).

[32] M. L. Mangano, M. Moretti, F. Piccinini, R. Pittau, and A. D. Polosa, JHEP **0307**, 001 (2003).

[33] T. Sjostrand, P. Eden, C. Friberg, L. Lonnblad, G. Miu, S. Mrenna, and E. Norrbin, Comput. Phys. Commun. **135**, 238 (2001).

[34] J. M. Campbell, R. K. Ellis, and C. Williams, Phys. Rev. D **81**, 074023 (2010).

[35] P. Z. Skands and D. Wicke, Eur. Phys. J. C **52**, 133 (2007).

[36] D. Wicke and P. Z. Skands, Nuovo Cim. B **123**, S1 (2008).